

## Appendix

### Appendix A Absorption and Outgassing Setup

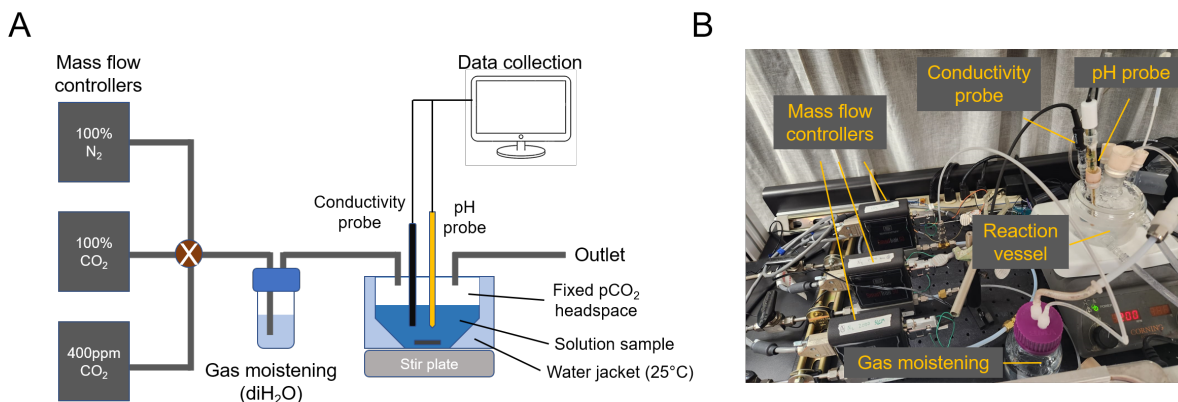


Figure A1: Absorption and outgassing setup.

### Appendix B Dissolved inorganic carbon equilibrium relations

First, it is worth understanding the pH dependence of the ACS, without any added acid-base species. The charge neutrality condition necessitates:

$$A = b + 2c + K_w/h - h \quad (\text{B1})$$

Here  $A$ ,  $b$ ,  $c$ , and  $h$  are the alkalinity, bicarbonate, carbonate, and proton concentrations, respectively, and the equilibrium relations between the DIC species are defined as follows:

$$H_{cp} = a/p_{CO_2} \quad (\text{B2})$$

$$K_1 = \frac{hb}{a} \quad (\text{B3})$$

$$K_2 = \frac{hc}{b} \quad (\text{B4})$$

Where  $a$  corresponds to the aqueous  $CO_2$  concentration and  $p_{CO_2}$  is the  $CO_2$  partial pressure of the gas in equilibrium with the solution. For an accurate treatment, the activity of the species must be considered, however, in this work, we assume dilute solution conditions to simplify the analysis. The conditions for  $CO_2$  capture in the ABCS take place roughly with pH between 9 and 11. Therefore, the hydroxide and proton concentrations are much smaller than the rest of the alkalinity and DIC species. Plugging in the DIC equilibrium relations, the above equation can be rewritten as a function of DIC concentration,  $C_{DIC}$ :

$$A = \frac{h/K_2 + 2}{\frac{h^2}{K_1 K_2} + \frac{h}{K_2} + 1} C_{DIC} = f_{DIC}(h) C_{DIC} \quad (\text{B5})$$

Here,  $f_{DIC}(h)$  is a function specific to the DIC system that relates alkalinity to  $C_{DIC}$  through the proton concentration. This allows for investigating the concentration perturbation, which can be mathematically written through the concentration factor,  $\chi$ . The concentration factor applies to all non-aqueous species in solution together:  $C_i = \chi C_{i,0}$ , where  $C_i$  is the concentration of species  $i$  in solution. Applying the concentration factor perturbation to the DIC system gives:

$$\frac{A}{C_{DIC}} = \frac{\chi A_0}{\chi C_{DIC,0}} = f_{DIC}(h) \quad (\text{B6})$$

This reveals that, because the  $\chi$  terms cancel out, pH is invariant to concentration factor in this regime. In fact, the solution  $\text{CO}_2$  partial pressure will increase linearly with  $\chi$ , but will not be further enhanced due to a shift in pH. The black line in Figure B1C confirms this derivation. In reality, the equilibrium relations,  $K_1$  and  $K_2$ , depend on the ionic strength and will result in a shift in pH as DIC solution is concentrated. Past analyses reveal that the ionic strength increases the outgassing efficiency by a factor of 30–50 % depending on the regime,<sup>22</sup> however, these effects are not considered in this work for simplicity.

## Appendix C Weak acid scaling relations

When the ratio of strong base to AH initial concentration is 1:1 (Fig. B1A), the pH increases for all reaction orders, but at varying rates, decreasing with higher reaction order. When the ratio of strong base to AH initial concentration is 1:2 (Fig. B1B), the pH first increases and then decreases as cooperative concentration effects begin to dominate. This non-monotonic effect is present only for reaction orders above 2. It further reveals that is possible to reach high pH regimes at lower concentrations, and then acidify a solution upon concentrating, which corresponds to the operating principle of ABCS.

Figure B1C-D plots the concentration pH dependence of a 1:1 and 1:2 strong base to weak acid solution with the DIC system added. This shows that at a given solution loaded with DIC at lower concentration, can be concentrated and acidified, thereby increasing the partial pressure of  $\text{CO}_2$ . Higher weak acid to base ratios increase acidification as a function of concentration, but also lower the concentration point at which the pH deviates from the strong base line. In general, this deviation is due to the fact that at low concentrations AH is entirely associated and uncharged, and so there is no anion to negate the strong base.

Finally, as with the alkalinity and DIC analysis in the previous section, a charge neutrality condition with the weak acid system can be analyzed:

$$[B^+] = [HCO_3^-] + 2[CO_3^{2-}] + [L_{n-1}A^-] + [OH^-] - [H^+] \quad (\text{C1})$$

In the conditions where hydroxide and proton concentrations are significantly smaller than those of the other non-conservative ions, the equation above simplifies to:

$$A = f_{DIC}(h)C_{DIC} + f_{a,n}(h)\alpha^n \quad (\text{C2})$$

Here,  $f_{a,n}(h)$  is a function specific to the  $n^{\text{th}}$  order condition relating the charge state of the acid to the pH of the solution, and  $\alpha$  is the total concentration of the weak acid, assuming that the non-charged species, L, is of equal concentration. Adding the concentration factor perturbation, a pH- $\chi$  dependence is revealed:

$$\frac{A_0 - f_{DIC}(h)C_{DIC,0}}{f_{a,n}(h)\alpha_0^n} = \chi^{n-1} \quad (\text{C3})$$

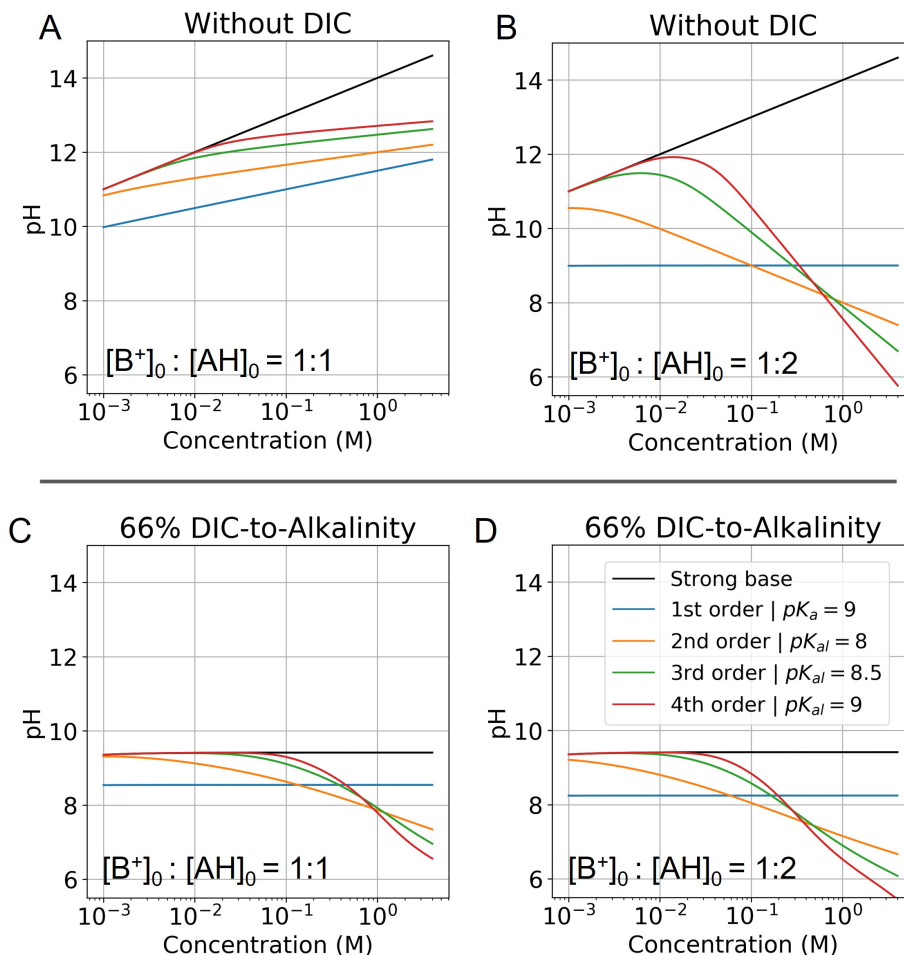


Figure B1: **Modelled pH as a function of fixed concentration.** Abscissa corresponds to the concentration of the strong base in solution, and is locked to the weak acid concentration based on the corresponding ratio. (A) pH of a solution with no DIC and a base to weak acid ratio of 1:1 is evaluated for different reaction orders (Table C1). (B) Same conditions, but at a base to weak acid ratio of 1:2 is plotted. (C) Same conditions as (A) are plotted, but with the addition of 66 % DIC relative to strong base concentration. (D) Same conditions as (B) are plotted, but with the addition of 66 % DIC relative to strong base concentration. Optimal  $K_{a,n}$  is picked for each reaction order based on optimization analysis in subsequent sections.

Inspecting the equations confirms the concentration-dependent pH effects that are the basis of the ABCS. Figure B1 plots the solution to the equation above for various parameter choices.

### C.1 Parameter space analysis and optimization

DIC-to-alkalinity diagram analysis in Figure C1, relating the DIC-to-alkalinity ratio, the alkalinity,  $CO_2$  partial pressure, and reaction order, allows for graphically understanding the possible concentration swing improvements at higher reaction orders. Each x-axis alkalinity value corresponds to an equivalent strong base concentration, and a fixed ratio of added weak acid (denoted in the bottom of each DIC-to-alkalinity diagram). In other words, at a 1:1 base to weak acid ratio, alkalinity of 0.1M corresponds to 0.1M of weak acid. A 1:2 ratio would imply that 0.1M of alkalinity corresponds to 0.2M of weak acid. This graphical representation projects to an ideal concentration step when moving right in a fixed DIC-to-alkalinity line, or dilution when moving left.

Table C1: Generalized reaction schemes.

Condition	Base	Acid	Reaction	Equilibrium relation	$\chi$ scaling at high conc.
Strong base	$B^+$	-	-	-	$\Delta \text{pH} \sim \log(\chi)$
1st order acid	-	AH	$AH \leftrightarrow A^- + H^+$	$K_{a,1} = \frac{[A^-][H^+]}{[AH]}$	$\Delta \text{pH} \sim -(1/2) * \log(\chi)$
2nd order acid	-	AH	$L + AH \leftrightarrow LA^- + H^+$	$K_{a,2} = \frac{[LA^-][H^+]}{[L][AH]}$	$\Delta \text{pH} \sim -\log(\chi)$
3rd order acid	-	AH	$2L + AH \leftrightarrow L_2A^- + H^+$	$K_{a,3} = \frac{[L_2A^-][H^+]}{[L]^2[AH]}$	$\Delta \text{pH} \sim -(3/2) * \log(\chi)$
$n^{\text{th}}$ order acid	-	AH	$(n-1)L + AH \leftrightarrow L_{n-1}A^- + H^+$	$K_{a,n} = \frac{[L_{n-1}A^-][H^+]}{[L]^{n-1}[AH]}$	$\Delta \text{pH} \sim -(n/2) * \log(\chi)$
Carbonate system	$\text{HCO}_3^-$	$\text{CO}_2(\text{aq})$	$\text{CO}_2(\text{aq}) + \text{H}_2\text{O} \leftrightarrow \text{HCO}_3^- + \text{H}^+$	$K_1 = \frac{[\text{HCO}_3^-][\text{H}^+]}{[\text{CO}_2(\text{aq})]}$	$\Delta \text{pH} \sim -(1/2) * \log(\chi)$
	$\text{CO}_3^{2-}$	$\text{HCO}_3^-$	$\text{HCO}_3^- \leftrightarrow \text{CO}_3^{2-} + \text{H}^+$	$K_2 = \frac{[\text{CO}_3^{2-}][\text{H}^+]}{[\text{HCO}_3^-]}$	$\Delta \text{pH} \sim -(1/2) * \log(\chi)$

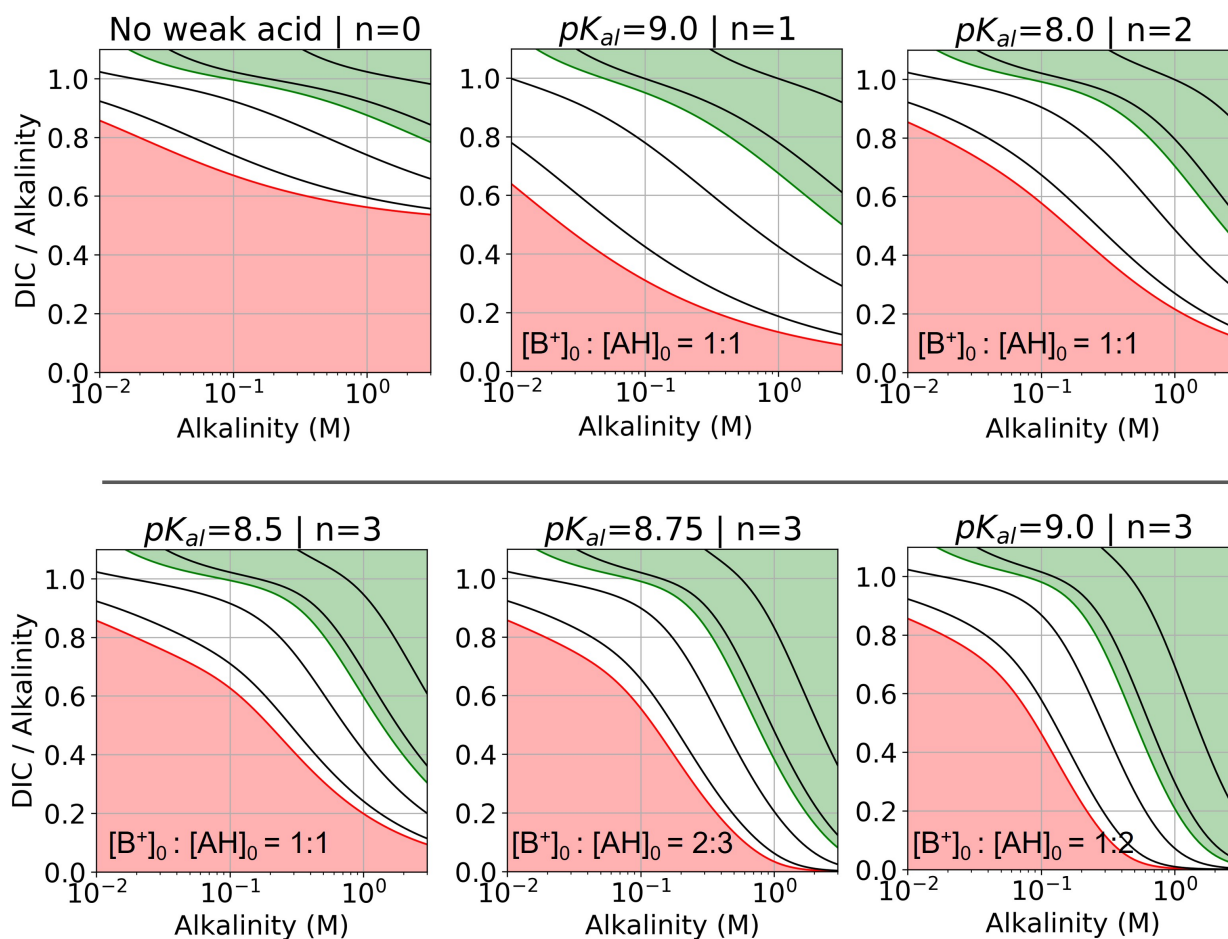


Figure C1: **DIC-to-alkalinity diagram for different reaction orders.** DIC-to-alkalinity is plotted as a function of initial strong base concentration, or equivalently  $[B^+]_0$ . The alkalinity to weak acid ratio is specified for each plot. Lines correspond to iso- $p\text{CO}_2$  values, with the red line corresponding to 0.4 mbar, and the green line corresponding to 50 mbar. Black lines from bottom up correspond to: 1, 10, 100, and 1000 mbar. Red region is eligible parameter space for absorption, and green region is eligible parameter space for outgassing (given the arbitrary choice of  $p_{out} = 50$  mbar). Optimal  $K_{a,n}$  are selected based on optimization analysis in Figure 3.

For all reaction orders, increasing alkalinity concentration results in increasing  $\text{CO}_2$  partial pressure (Fig. C1). However, higher order reactions compress the iso- $\text{pCO}_2$  lines as a function of concentration, which results in a relatively higher partial pressure increase. At higher alkalinity (above 0.1 M), higher reaction orders lowers the DIC-to-alkalinity ratio at 50 mbar (green line), which implies that even more  $\text{CO}_2$  can be outgassed upon concentration if the same amount of DIC is loaded into solution. Higher weak acid to alkalinity ratios result in further compressing of the iso- $\text{pCO}_2$  lines and lowering the DIC-to-alkalinity ratio at 50 mbar (green line) at high concentrations. The  $\text{p}K_{a,n}$  values for the DIC-to-alkalinity diagrams in Figure C1 were chosen based on an analysis of optimal  $C_{out}$  conditions.

Figure C2 plots  $C_{out}$ ,  $\text{p}CO_2^{max}$ , and  $\text{p}H_4$  (pre-absorption pH), as functions of  $K_{a,n}$  and initial strong base concentration,  $[\text{B}^+]_0$ . By evaluating this parameter landscape, an optimal  $\text{p}K_{a,n}$  and  $[\text{B}^+]_0$  can be chosen to maximize the cycle capacity,  $C_{out}$ . Plots A, B, C, and D in Figure C2 correspond to first, second, third, and fourth order reactions at a 1:1 base to weak acid ratio. The red dot corresponds to the optimal parameter point where the process has the largest cycle capacity, revealing the trade-off between maximum  $C_{out}$  and absorption rate, which is captured by the  $\text{p}H_4$  metric.  $[\text{B}^+]_0$  values that are lower than the optimal red point, can increase the post-outgassing pH by a unit or more, while decreasing the  $C_{out}$  value.

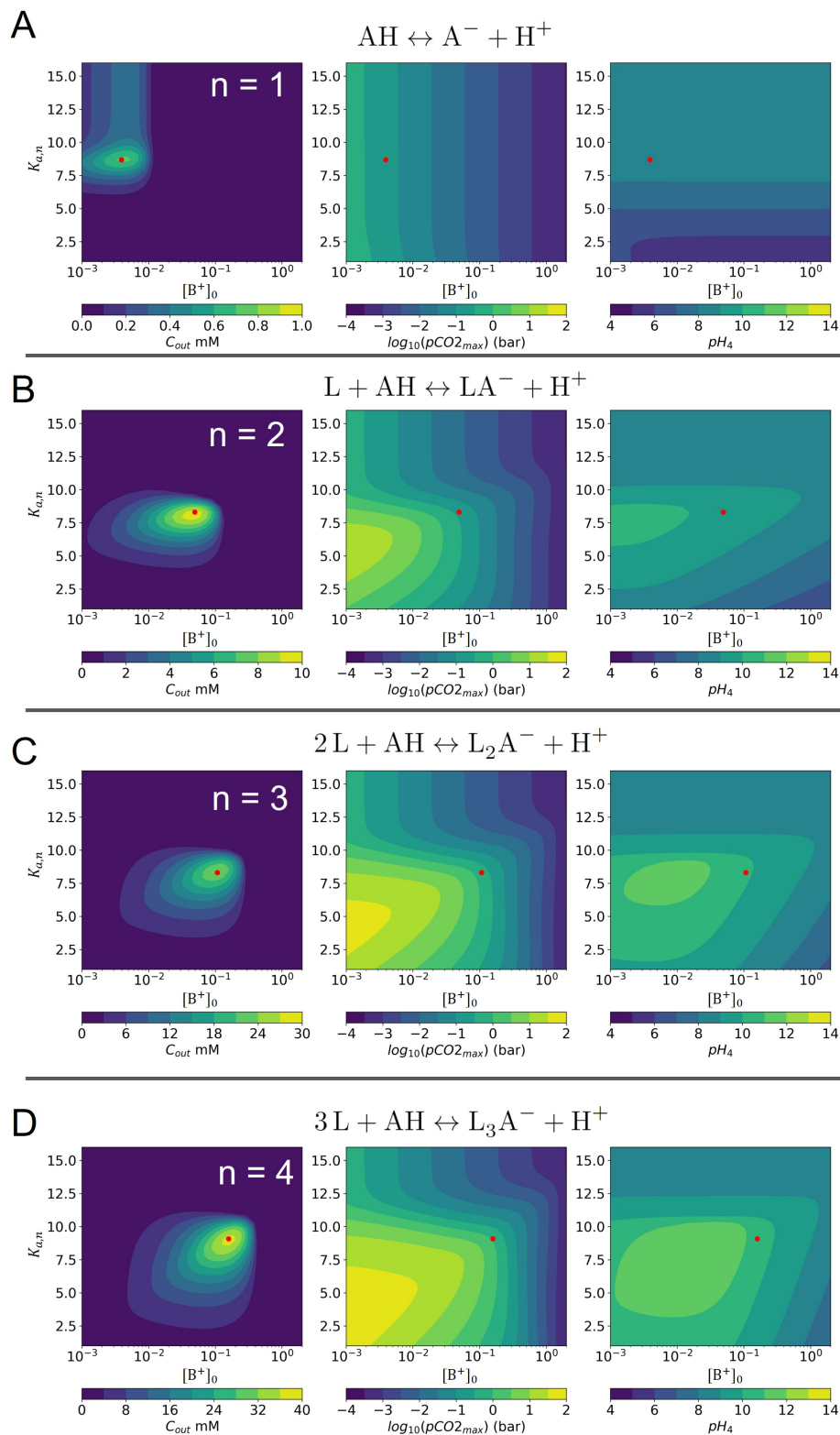


Figure C2: **ABCS output parameter plot**. Each point calculates the output from a theoretical ABCS process with corresponding parameters. Contour plots report the  $C_{out}$  (left),  $p_{CO_2}^{max}$  (middle), and  $pH_4$  (right), as a function of  $K_{a,n}$  and initial strong base concentration,  $[B^+]_0$ . For each point,  $p_{in} = 0.3$  mbar,  $p_{out} = 50$  mbar, and final alkalinity is 2 M. A, B, C, and D correspond to first, second, third, and fourth order reaction conditions; the red dot in each plot corresponds to the optimal  $K_{a,n}$  and  $[B^+]_0$  value that maximizes  $C_{out}$ .